Supplementary Information

Large-scale Evaluation of Cascaded Adsorption Heat Pumps Based on Metal/Covalent Organic Frameworks

Wei Li, [1,#] Xiaoxiao Xia [1,#] and Song Li [1,2,3*]

[1]State Key Laboratory of Coal Combustion, School of Energy and Power Engineering, Huazhong University of Science and Technology, Wuhan 430074, China

[2]China-EU Institute for Clean and Renewable Energy, Huazhong University of Science and Technology, Wuhan 430074, China

[3]Nano Interface Centre for Energy, School of Energy and Power Engineering, Huazhong University of Science and Technology, Wuhan 430074, China

Table of Contents

Contents	Page Number
S1. Computation details of COP_C for cascaded AHPs	**2**
S2. Top-performing adsorbents of LS and HS in cascaded AHPs	**3-6**
S3. Structure-property relationship	**7-10**
S4. Evolution trend of screening and isotherms of top-performing structures	**11-16**
S5. Experimental synthesis, characterization and vapor adsorption	**17-19**
S6. Data mining and machine learning	**20-22**

S1. Computaion details of COP_C for cascaded AHPs

The overall COP_C of a cascaded AHP is defined as:

$$COP_C = \frac{Q_{HS}}{Q_{LS}} COP_{C,\,LS} + COP_{C,\,HS} \qquad \text{* MERGEFORMAT (S1)}$$

The Q_{HS} is the heat obtained from the HS during adsorption, Q_{LS} is the energy required for regeneration of adsorbents in the LS, $COP_{C,\,LS}$ and $COP_{C,\,HS}$ are the COP_C of LS and HS, respectively. In this work, it is assumed that Q_{HS} equals to Q_{LS} , suggesting that the energy generated from HS during adsorption is completely used for adsorbent regeneration of LS.[1, 2]

Table S1. TraPPE force field parameters of ethanol.

adsorbate	interaction site	σ (Å)	ε/k_B (K)	q (e)
ethanol	CH_3	3.75	98.0	0
	CH_2	3.95	46.0	0.265
	O	3.02	93.0	-0.7
	H	0	0	0.435

S2. Top-performing adsorbents of LS and HS in cascaded AHPs

Table S2. The selected top-performing MOFs in LS.

Ref code	LCD (Å)	V_a (cm^3/g)	ASA (m^2/g)	K_H (mol/kg·Pa)	COP_C
PEVQEO	14.87	1.23	3587	5.26×10^{-5}	0.93
XEBHOC	12.36	1.66	4604	1.68×10^{-4}	0.89
XAWVUN	10.48	1.65	4693	1.46×10^{-4}	0.87
IRMOF-6	15.72	1.07	3175	1.07×10^{-4}	0.86
RUVKAV	11.94	1.22	3625	2.37×10^{-4}	0.83
MIL-88C-open	13.74	1.42	3909	1.08×10^{-3}	0.82
FEFDEB	13.11	1.31	3488	3.42×10^{-4}	0.82
LUYHAP	12.04	1.15	3563	2.80×10^{-4}	0.82
FUNCEX	13.22	1.30	3491	3.51×10^{-3}	0.82
ECOLEP	11.30	2.07	4555	7.80×10^{-2}	0.81

Table S3. The selected top-performing COFs in LS.

COF name	LCD (Å)	V_a (cm^3/g)	ASA (m^2/g)	K_H (mol/kg·Pa)	COP_C
ILCOF-1-AB	11.09	2.42	6714	7.99×10^{-5}	0.96
TpFn	22.86	1.20	1717	4.65×10^{-5}	0.88
TT-COF	26.31	1.30	1610	2.14×10^{-4}	0.88
TpBD	22.86	1.20	1717	2.65×10^{-4}	0.88
IISERP-COF3	20.05	1.10	1705	9.66×10^{-5}	0.87
TpPa-1	16.14	0.93	1643	1.44×10^{-4}	0.87
Py-Azine COF	13.02	1.11	2031	8.54×10^{-5}	0.87
MC-COF-TP-E22E31	25.10	1.26	1660	3.94×10^{-5}	0.87
MC-COF-TP-E11E22	20.15	1.19	1730	9.26×10^{-5}	0.86
TPBD-ME2	21.64	1.03	1523	2.14×10^{-4}	0.86
HO2C-H2P-COF	10.89	1.90	4927	1.15×10^{-2}	0.85
Py-1P COF	18.66	1.34	2154	5.08×10^{-5}	0.85
MC-COF-TP-E12E21	19.96	1.14	1674	2.48×10^{-2}	0.85
MC-COF-NiPc-E1E7	15.08	0.88	1462	1.07×10^{-4}	0.85
COF-5	23.66	1.24	1707	2.72×10^{-4}	0.84
MC-COF-TP-E1E3E7	22.70	1.39	1808	1.43×10^{-5}	0.84
TzDa	29.23	1.68	2027	2.75×10^{-5}	0.84
MC-COF-TP-E12E71	21.95	1.36	1769	1.74×10^{-2}	0.84
BF-COF-1	13.26	1.96	5097	4.73×10^{-4}	0.84
TpPa-SO3H-Py	16.32	0.83	1523	2.34×10^{-4}	0.83
MC-COF-TP-E22E41	22.92	1.19	1691	3.40×10^{-3}	0.83
BDT-COF	30.00	1.54	1797	4.03×10^{-4}	0.82
BCCTP-COF	16.89	1.04	1722	7.16×10^{-5}	0.82
TBPB COF	16.69	0.98	1677	8.13×10^{-5}	0.82
Pc-PBBA-COF	16.84	0.81	1391	1.81×10^{-4}	0.81
Py-DBA-COF-2	38.29	2.06	1973	1.73×10^{-5}	0.81

MC-COF-TP-E11E71	25.19	1.39	1824	7.49×10^{-5}	0.81
DA-COF	19.39	1.08	1646	2.72×10^{-4}	0.80
TpBD-NO2	21.41	0.98	1517	6.00×10^{-4}	0.79
CuP-SQ COF	12.91	1.46	3240	1.67	0.79
Tp-Por COF-AB	20.14	1.73	2880	4.07×10^{-4}	0.79
POR-COF	14.05	1.54	3548	1.98×10^{-2}	0.78
TpBD-2NO2	21.72	1.13	1638	3.49×10^{-4}	0.78
MC-COF-TP-E11E72	24.94	1.45	1884	1.15×10^{-4}	0.76
COF-66	27.00	3.06	4453	2.69×10^{-5}	0.75
Py-An COF	19.55	1.47	2344	1.93×10^{-4}	0.75

Table S4. The selected top-performing MOFs in HS.

Ref code	LCD (Å)	V_a (cm^3/g)	ASA (m^2/g)	K_H (mol/kg·Pa)	COP_C
COJHIT	10.05	0.83	2286	1.03×10^{-3}	0.85
IVETOT	10.10	0.80	2417	6.68×10^{-4}	0.84
FAKLIO	9.33	0.69	2094	3.78×10^{-4}	0.84
SOHGUS	9.42	0.77	2327	8.24×10^{-4}	0.84
MOCKAR	10.82	0.91	2957	6.61×10^{-4}	0.83
ANUGUM	8.63	0.98	3514	1.42×10^{-3}	0.83
FAKMAH	8.52	0.66	2086	6.37×10^{-4}	0.81
WIYFAM	9.66	0.76	2810	1.23×10^{-3}	0.80
MATVEJ	8.87	0.79	2986	2.07×10^{-3}	0.79
FAKLOU	9.11	0.58	1730	4.04×10^{-4}	0.79
YILJAG	9.73	0.75	2785	1.44×10^{-3}	0.79
VEXVAW	9.77	0.68	2551	1.92×10^{-3}	0.78
HOGLEV01	10.39	0.70	2580	6.44×10^{-3}	0.77
NEDWAW	8.28	0.71	2535	2.38×10^{-3}	0.77
OYEJOS	9.85	0.53	1890	6.75×10^{-4}	0.76
ZIKJIO	7.32	0.74	2884	3.23×10^{-3}	0.76
XUGSEY	7.34	0.85	3379	9.00×10^{-3}	0.75
KIGCEK	10.57	0.41	1226	4.13×10^{-4}	0.75
BEPRIZ	10.21	0.71	2539	1.72×10^{-3}	0.75
LASYOU	10.03	0.65	2267	1.32×10^{-3}	0.75
WEBKOF	10.38	0.72	2644	3.06×10^{-3}	0.75
OQETEK	9.23	0.61	2009	1.42×10^{-3}	0.74
ALAMUW	11.50	1.06	3529	1.37×10^{-3}	0.74
QUQPOI	6.08	0.68	2599	2.10×10^{-3}	0.74
LEDLEN	8.15	0.55	2033	2.08×10^{-3}	0.74
CEKHIL	9.32	1.16	4266	3.93×10^{-3}	0.73
ALULAV	8.90	1.24	5006	7.61×10^{3}	0.73
SUTBIT	8.24	0.58	1823	1.70×10^{-3}	0.73
EDOMAM	8.35	0.65	2369	3.68×10^{-3}	0.73
PARNIH	8.34	0.59	2204	1.21×10^{-3}	0.73

FEFCUQ	8.96	0.69	2502	4.90×10^{-3}	0.72
ZnBDCdabco	9.39	0.70	2196	7.98×10^{-4}	0.72
GACQAE	8.82	0.65	2129	3.57×10^{-3}	0.72
BUVYIB	11.54	0.77	2649	9.27×10^{-3}	0.72
ALUKIC	8.97	1.30	5204	1.09×10^{3}	0.71
ODIXEG	10.41	1.32	4098	4.76×10^{-3}	0.71
RAXCOK	7.28	0.76	3182	6.61×10^{-3}	0.71
TERFUT	8.07	0.57	1977	4.66×10^{-3}	0.71
OBEDEE	5.86	0.43	1672	1.81×10^{-3}	0.71
FEHCOM	7.63	0.42	1492	7.98×10^{-4}	0.70
MOYYEF	7.43	0.52	1862	2.71×10^{-3}	0.70
HIHNUJ	7.99	0.80	2746	7.28×10^{-3}	0.70
MOCKEV	10.89	0.87	2869	1.02×10^{-2}	0.69
PARNON	7.82	0.48	1891	3.09×10^{-3}	0.69
ICALOP	7.82	0.79	2916	2.59×10^{-2}	0.68
SENWAL	8.58	1.00	3118	1.06×10^{-1}	0.68
RIBDAJ	5.82	0.59	2342	3.38×10^{-3}	0.68
VEJYIT01	6.61	0.52	1909	3.10×10^{-3}	0.68
RIBDEN	5.92	0.59	2273	3.80×10^{-3}	0.68
EXEQII	7.21	0.45	1392	1.87×10^{-3}	0.68
ICAGOK	9.13	0.57	2122	9.37×10^{-3}	0.68
AVELOD	8.08	0.45	1678	3.64×10^{-3}	0.68
SAQQIL	11.46	0.60	1766	8.54×10^{-3}	0.68
AVEMAQ	7.91	0.41	1682	1.51×10^{-3}	0.68
VEJYIT	6.44	0.50	1889	3.93×10^{-3}	0.68
BEPROF	7.99	0.77	3039	1.09×10^{-2}	0.67
KEFBOO	12.62	0.94	3062	3.74×10^{-2}	0.67
TERFIH	8.72	0.39	1397	2.23×10^{-3}	0.67
AFOYOK	8.04	0.38	1394	6.91×10^{-4}	0.67
NEJYUY	6.67	0.43	1835	8.82×10^{-3}	0.67
ZnMOF-74	11.89	0.51	1278	2.31×10^{-3}	0.66
FEFDAX	7.82	0.64	2346	1.98×10^{-2}	0.66
GERWEH	9.32	0.39	1217	1.40×10^{-3}	0.65
NEDWEA	7.53	0.59	2256	1.25×10^{-1}	0.65
IDIWOH01	7.49	0.48	1568	3.26×10^{-3}	0.65
WAJJAU	7.49	0.33	1024	7.96×10^{-4}	0.65

Table S5. The selected top-performing COFs in HS.

COF name	LCD (Å)	V_a (cm^3/g)	ASA (m^2/g)	K_H (mol/kg·Pa)	COP_C
COF-102	9.04	1.86	5129	3.98×10^{-3}	0.80
COF-103	9.68	2.05	5315	1.94×10^{-3}	0.73
MPCOF	10.27	0.66	1394	1.56×10^{-4}	0.73
DL-COF-2-bor	25.09	4.82	6505	1.37×10^{-5}	0.71

CuP-TFPh COF	19.04	2.07	4439	6.22	0.66
T-COF 1	8.18	0.48	1045	4.05×10^{-4}	0.65
DL-COF-2-ctn	16.19	4.29	6655	1.11×10^{-3}	0.64
BLP-2H-AA	9.50	0.56	1115	4.57×10^{-4}	0.64

S3. Structure-property relationship

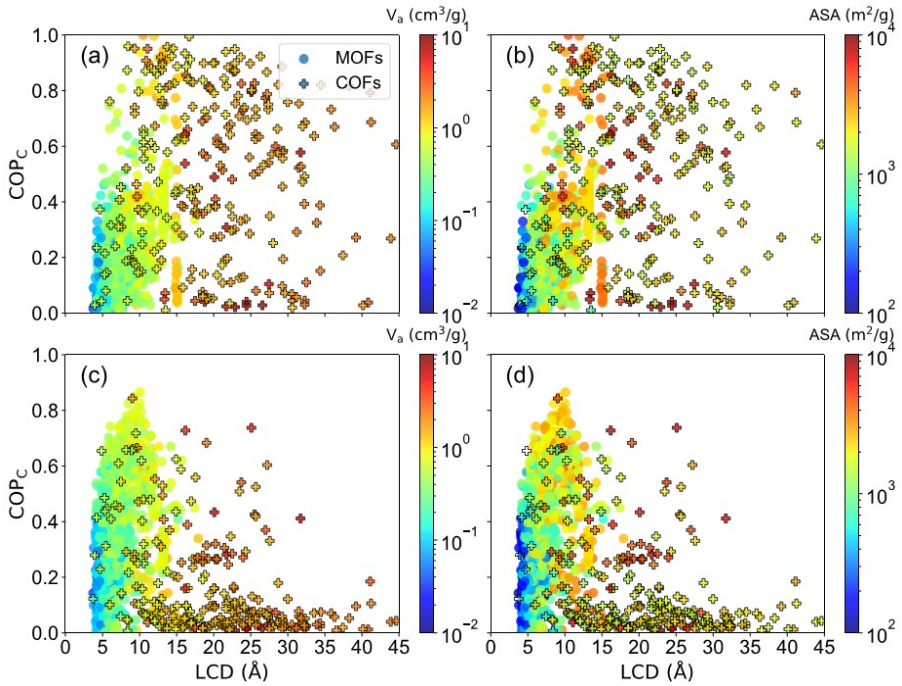

Fig. S1 The correlation between LCD and COP_C in the (a) LS, colored by V_a, (b) LS, colored by ASA, (c) HS, colored by V_a, (d) HS, colored by ASA.

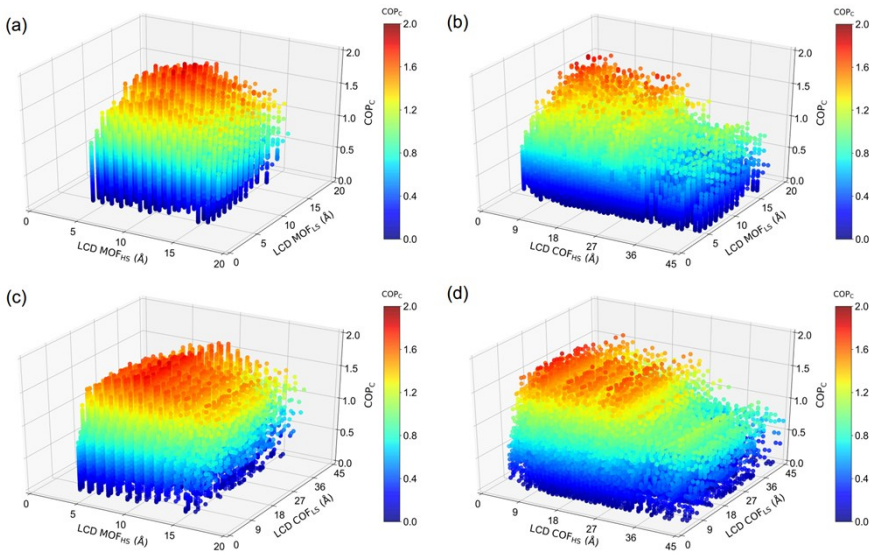

Fig. S2 The relationship between LCD_{LS}, LCD_{HS} and COP_C, colored by COP_C, if i-0.5 < LCD ≤ i+0.5, the LCD are set as i. (a) Type 1: MOFs for LS and HS (MOF_{LS} + MOF_{HS}). (b) Type 2: MOFs for LS and COFs for HS (MOF_{LS} + COF_{HS}). (c) Type 3: COFs for LS and MOFs for HS (COF_{LS} + MOF_{HS}). (d) Type 4: COF for LS and HS (COF_{LS} + COF_{HS}).

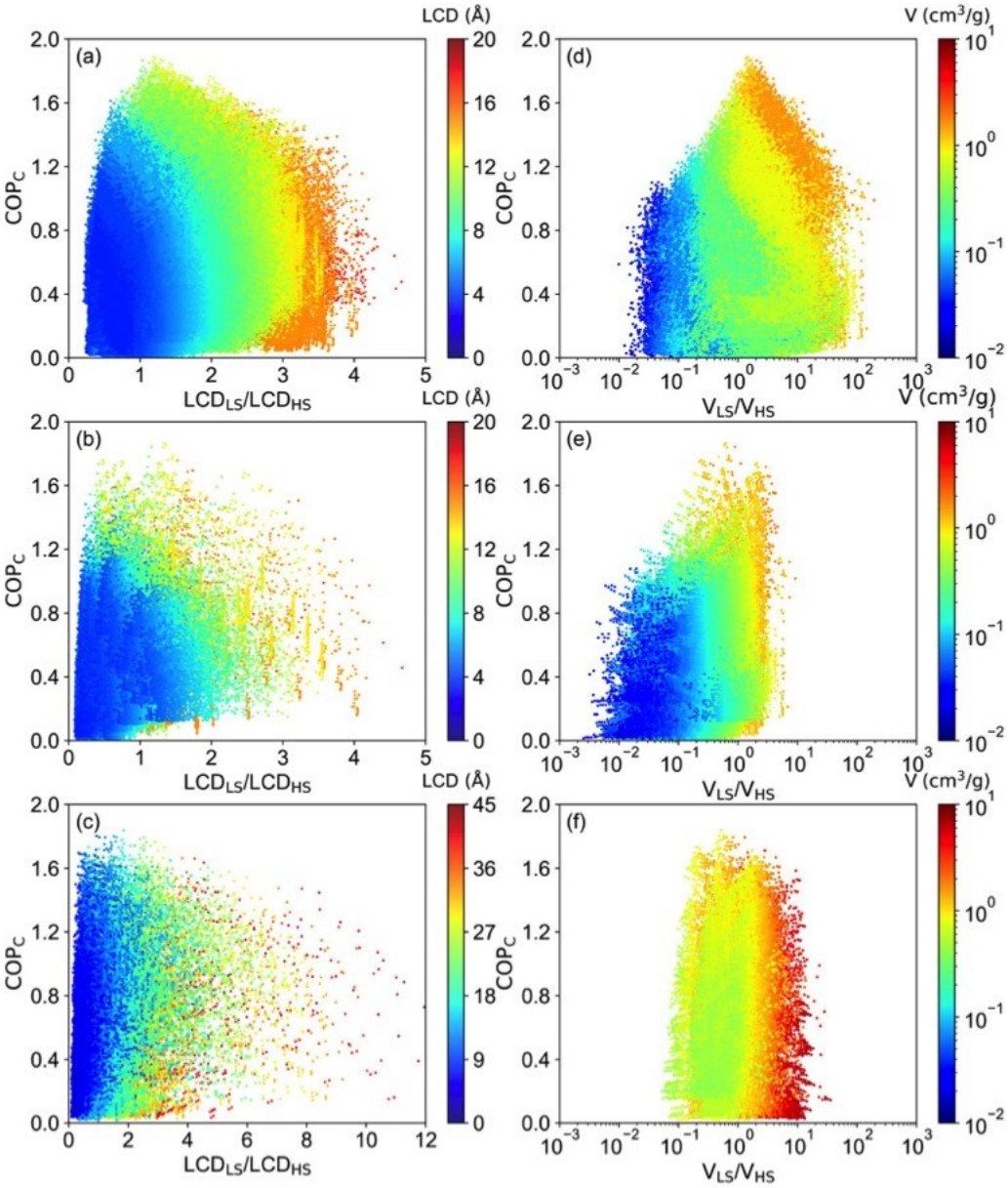

Fig. S3 The relationship between LCD_{LS}/LCD_{HS} and COP_C, colored by the LCD in LS, (a) Type 1: MOFs for LS and HS (MOF_{LS} + MOF_{HS}). (b) Type 2: MOFs for LS and COFs for HS (MOF_{LS} + COF_{HS}). (c)Type 4: COF for LS and HS (COF_{LS} + COF_{HS}). The relationship between $V_{a,\ LS}/V_{a,\ HS}$ and COP_C, colored by the V_a in the LS, (d) Type 1: MOFs for LS and HS (MOF_{LS} + MOF_{HS}). (e) Type 2: MOFs for LS and COFs for HS (MOF_{LS} + COF_{HS}). (f) Type 4: COF for LS and HS (COF_{LS} + COF_{HS}).

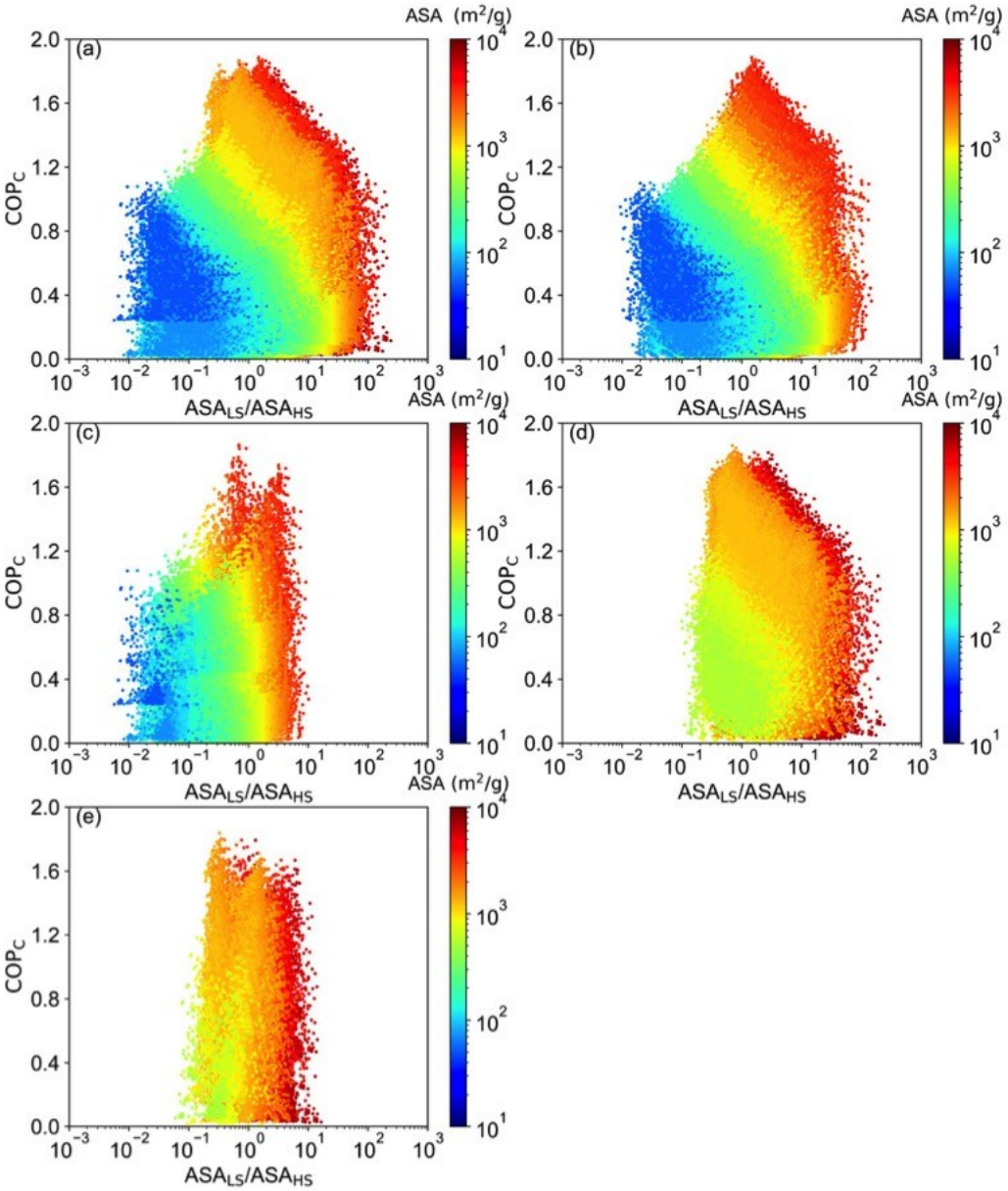

Fig. S4 The relationship between ASA_{LS}/ASA_{HS} and COP_C, colored by ASA in the LS. (a) All the 3 166 602 cascaded AHPs. (b) Type 1: MOFs for LS and HS (MOF_{LS} + MOF_{HS}). (c) Type 2: MOFs for LS and COFs for HS (MOF_{LS} + COF_{HS}).(d) Type 3: COFs for LS and MOFs for HS (COF_{LS} + MOF_{HS}) (e)Type 4: COF for LS and HS (COF_{LS} + COF_{HS}).

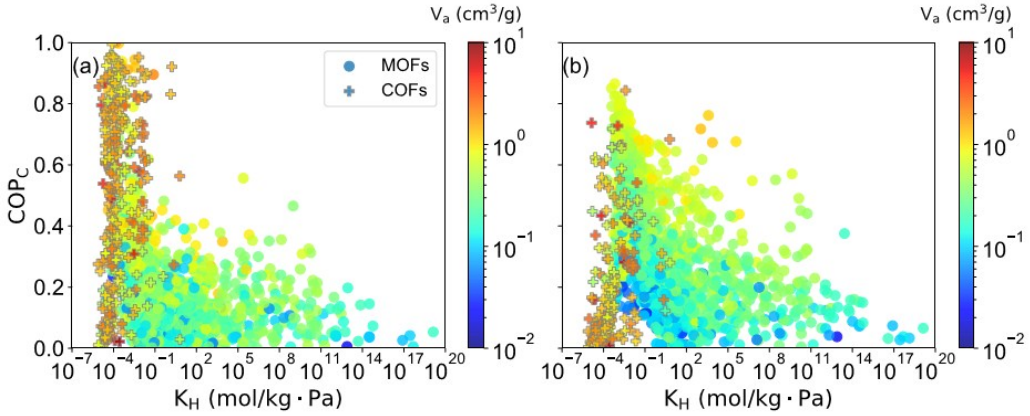

Fig. S5 The relationship between COP_C and Henry's constant (K_H) in the (a) LS, (b) HS, colored by V_a.

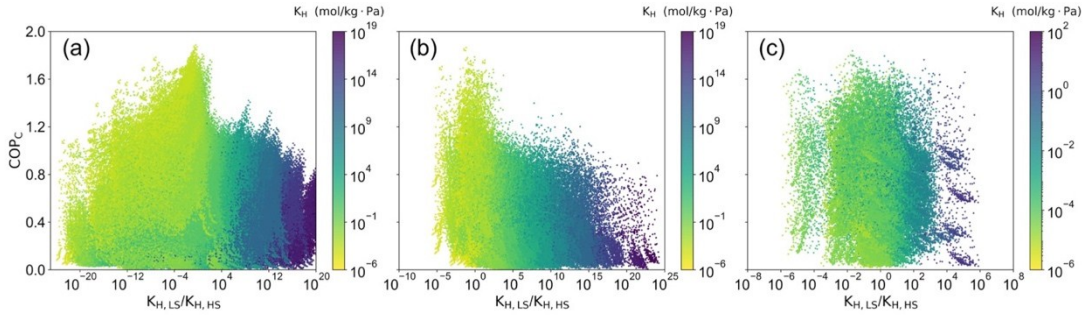

Fig. S6 The COP_C distribution of cascaded AHPs with the various $K_{H,LS}/K_{H,HS}$. (a) Type 1: MOFs for LS and HS (MOF_{LS} + MOF_{HS}). (b) Type 2: MOFs for LS and COFs for HS (MOF_{LS} + COF_{HS}). (c)Type 4: COF for LS and HS (COF_{LS} + COF_{HS}).

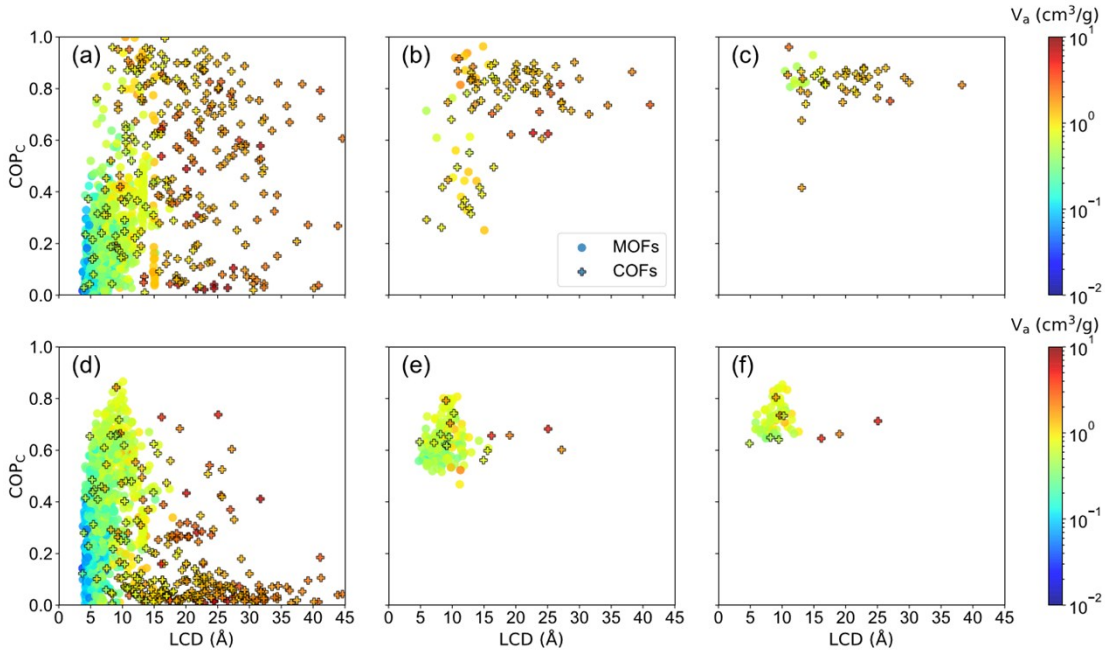

Fig. S7 The structure-property relationship of the MOFs and COFs in (a) LS of the first round, (b) LS of the second round, (c) LS of the third round, (d) HS of the first round, (e) HS of the second round, (f) HS

of the third round.

S4. Evolution trend of screening and isotherms of top-performing structures

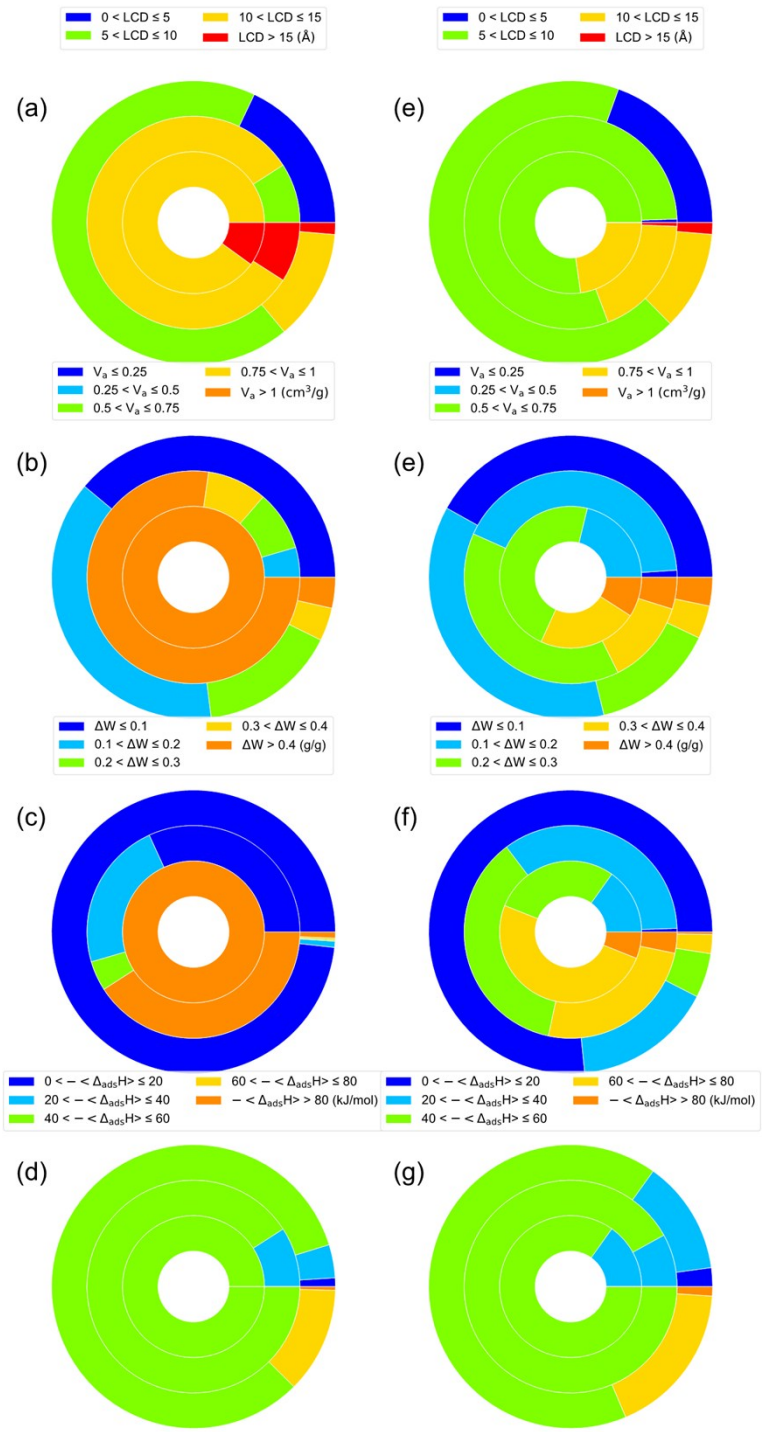

Fig. S8 The evolutionary trend of MOFs in LS and HS from high-throughput computational screening. The evolutionary trend of (a) LCD (b) V_a (c) ΔW (d) -<Δ_{ads}H> from the first, second and third rounds of screening (from the outer to the inner) in LS. The number of MOFs in the first, second and third round of screening are 1426, 22 and 10. The evolutionary trend of (d) LCD (e) V_a (f) ΔW (g) -<Δ_{ads}H> from the first, second and third rounds of screening (from the outer to the inner) in HS. The number of MOFs in

the first, second and third round of screening are 1593, 187 and 66, respectively.

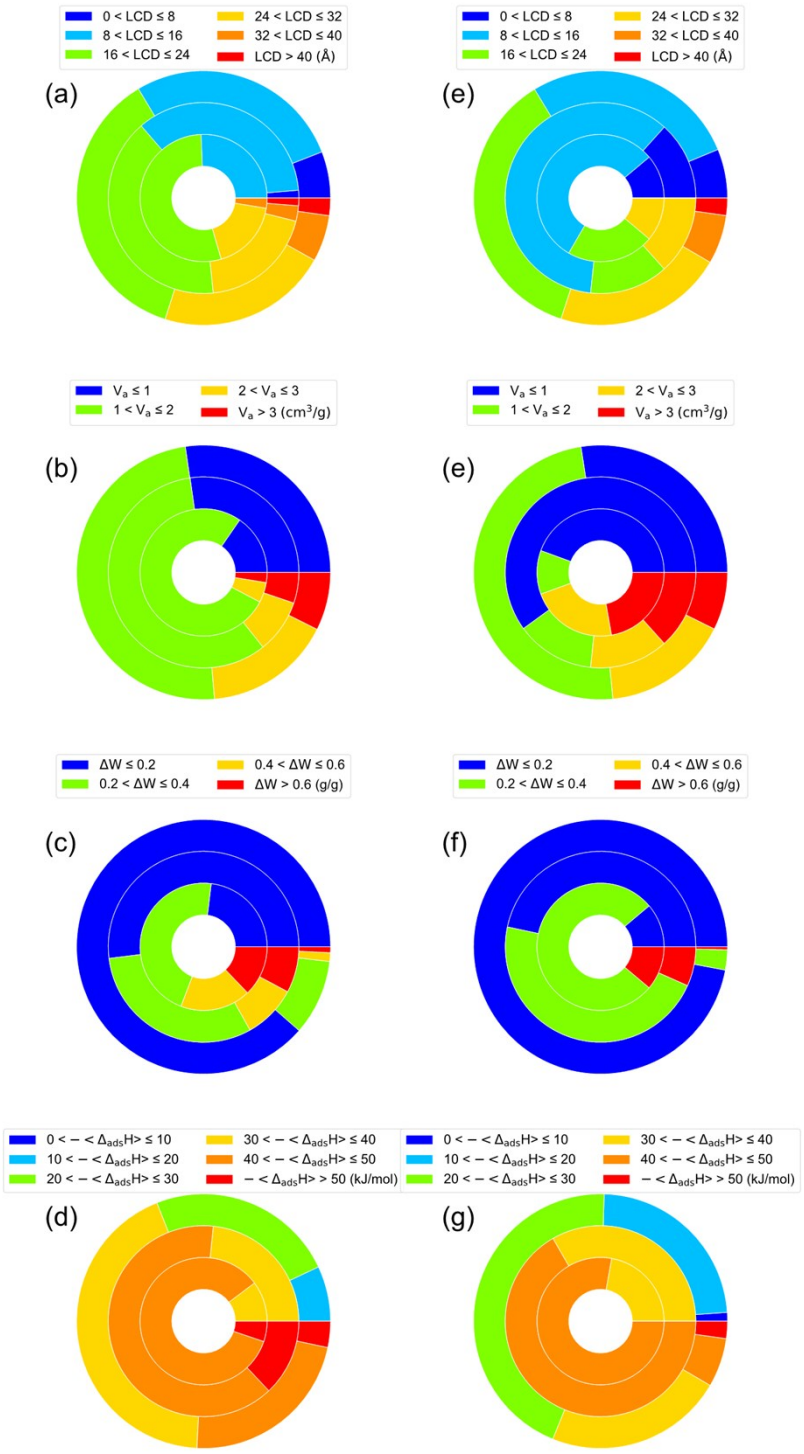

Fig. S9 The evolutionary trend of COFs in LS and HS from high-throughput computational screening. The evolutionary trend of (a) LCD (b) V_a (c) ΔW (d) -<Δ_{ads}H> from the first, second and third rounds of screening (from the outer to the inner) in LS. The number of COFs in the first, second and third round of screening are 271, 77 and 39. The evolutionary trend of (d) LCD (e) V_a (f) ΔW (g) -<Δ_{ads}H> from the first, second and third rounds of screening (from the outer to the inner) in HS. The number of COFs in the first, second and third round of screening are 273, 15 and 9, respectively.

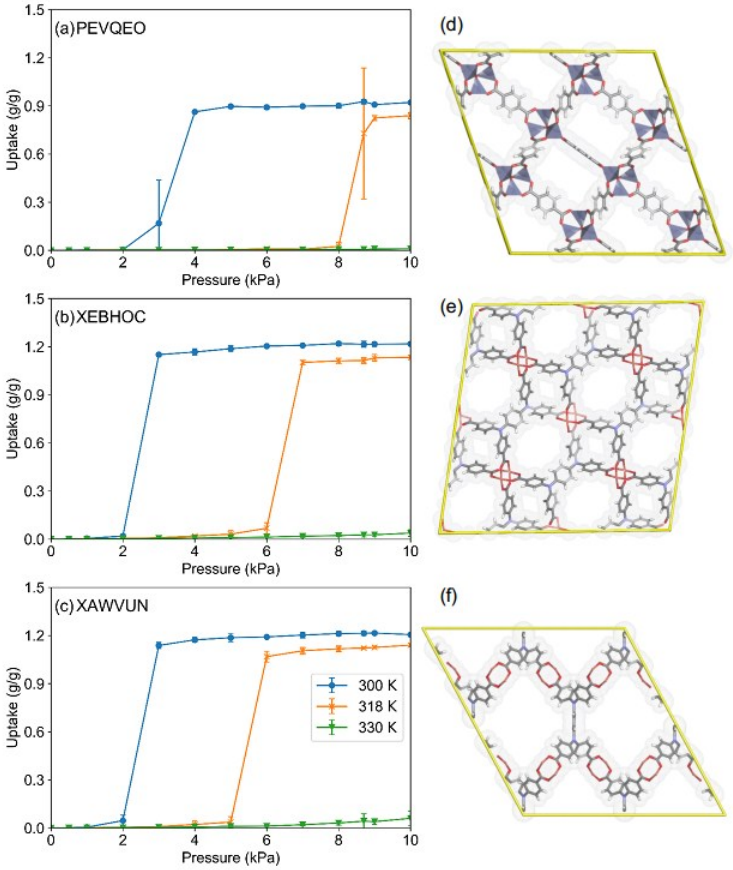

Fig. S10 Ethanol adsorption isotherm of the selected top three MOFs in the LS. (a) PEVQEO, (b) XEBHOC and (c) XAWVUN at 300 K, 318 K and 330 K, and the corresponding crystal structures of (d) PEVQEO, (e) XEBHOC and (f) XAWVUN.

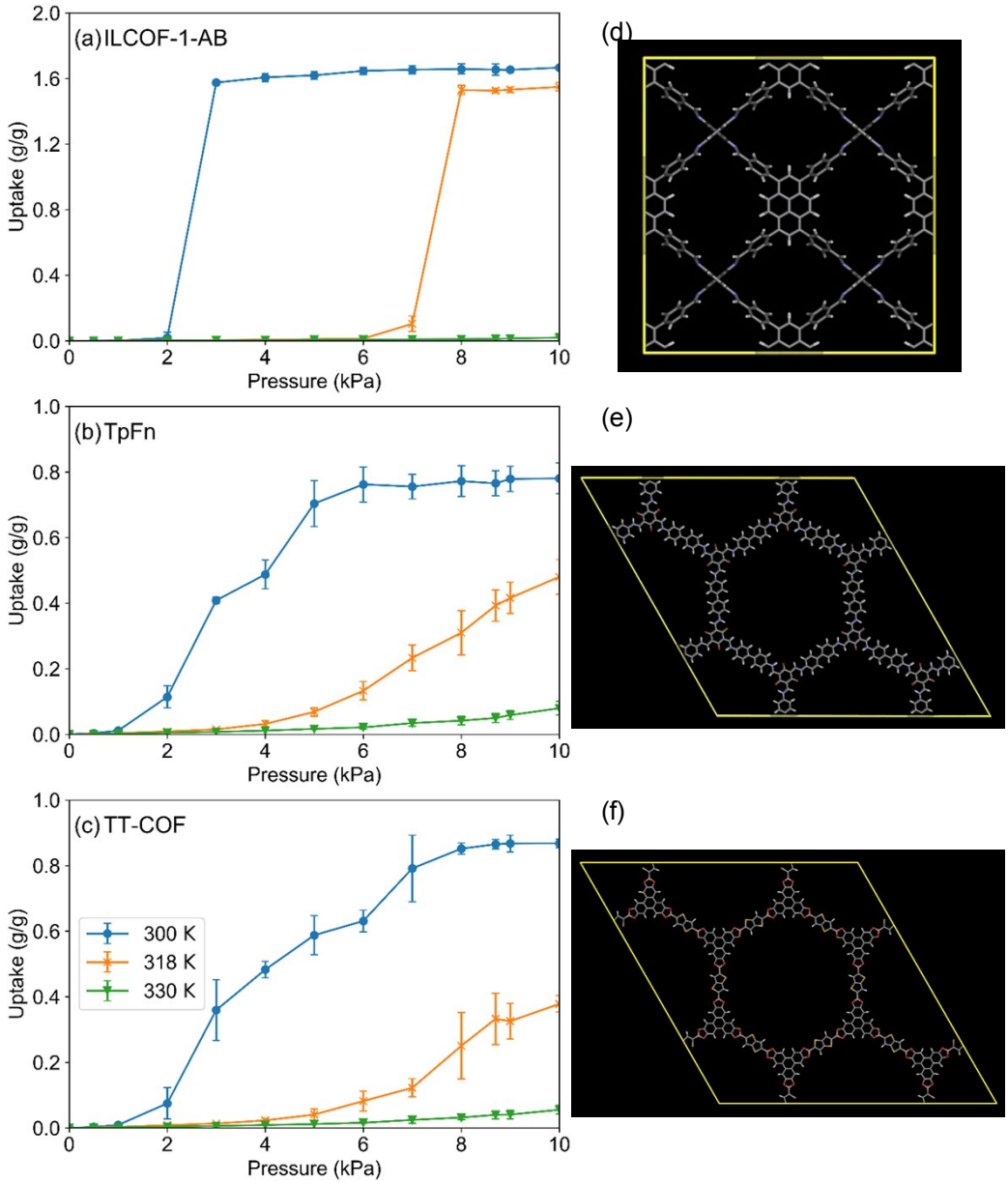

Fig. S11 Ethanol adsorption isotherm of the selected top three COFs in the LS. (a) ILCOF-1-AB, (b) TpFn and (c) TT-COF at 300 K, 318 K and 330 K, and the corresponding crystal structures of (d) ILCOF-1-AB, (e) TpFn and (f) TT-COF.

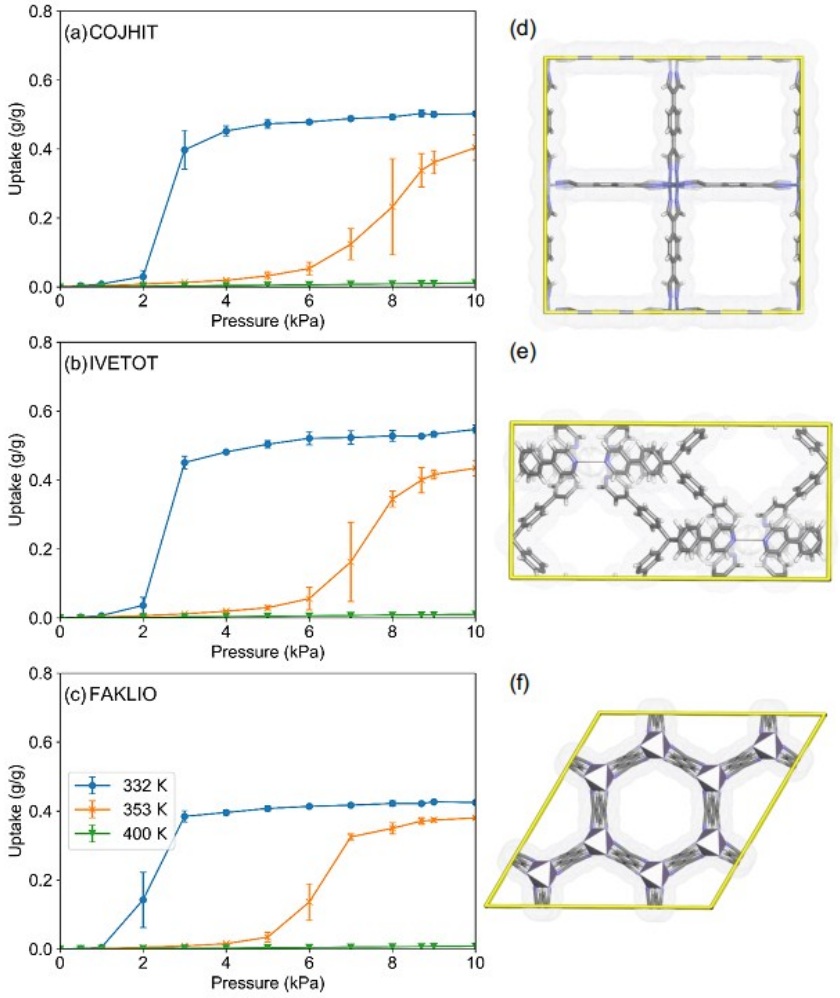

Fig. S12 Ethanol adsorption isotherm of the selected top three MOFs in the HS. (a) COJHIT, (b) IVETOT and (c) FAKLIO at 332 K, 353 K and 400 K, and the corresponding crystal structures of (d) COJHIT, (e) IVETOT and (f) FAKLIO.

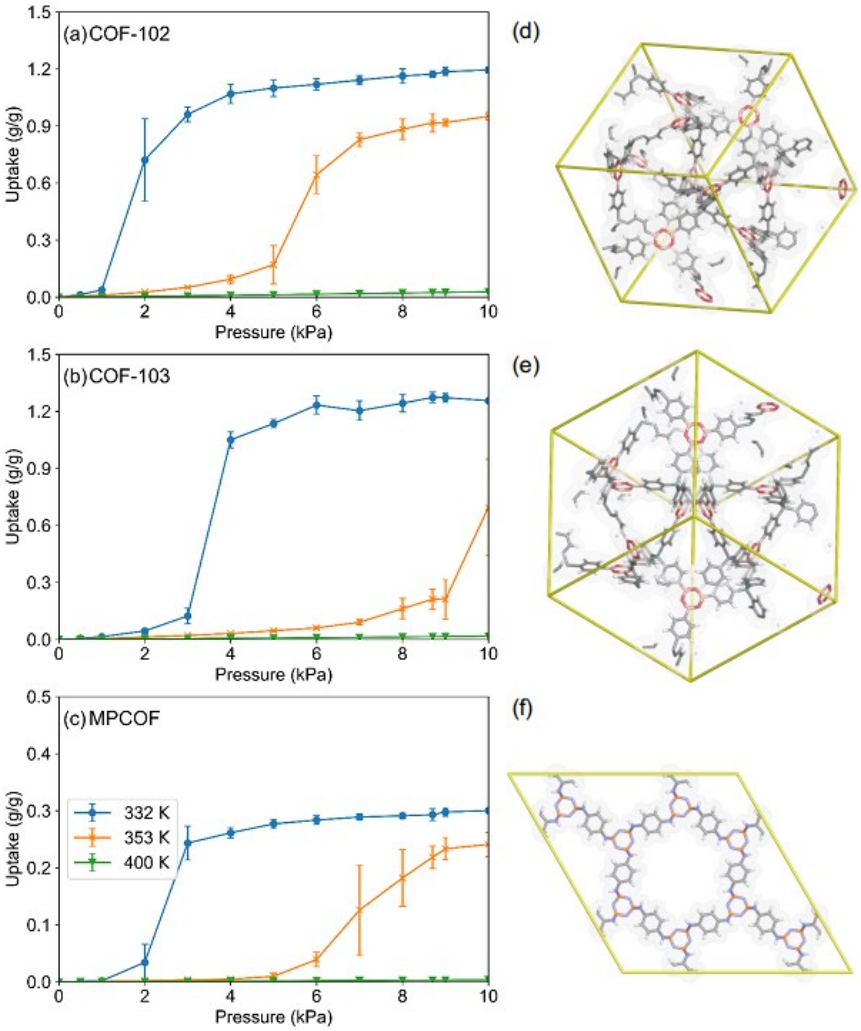

Fig. S13 Ethanol adsorption isotherm of the selected top three COFs in the HS. (a) COF-102, (b) COF-103 and (c) MPCOF at 332 K, 353 K and 400 K, and the corresponding crystal structures of (d) COF-102, (e) COF-103 and (f) MPCOF.

S5. Experimental synthesis, characterization and vapor adsorption

Materials. All chemicals required in this study were purchased from commercial sources and used without any further purification. 2,3,6,7,10,11-hexahydroxytriphenylene (HHTP, 96 %) from Zhengzhou Alfachem Co., Ltd. 1,4-benzene diboronic acid (BDBA, 97 %), copper nitrate trihydrate ($Cu(NO_3)_2 \cdot 3H_2O$, 99 %), trimesic acid (H_3BTC, 97 %), Chromium(III) nitrate nonahydrate ($Cr(NO_3)_3 \cdot 9H_2O$, 99 %) and terephthalic acid (H_2BDC, 99 %) from Shanghai Aladdin Bio-Chem Technology Co., Ltd. Absolute ethanol, methanol, acetone, glacial acetic acid and N,N-dimethylformamide (DMF, 99.5 %) from Sinopharm Chemical Reagent Co., Ltd. (Shanghai, China, AR). Nitrogen (N2, 99.999 %) and helium (He, 99.999 %) gases from Huaerwen Industrial Co., Ltd.

Synthesis of COF-1. COF-1 was synthesized using a slightly modified method with previously reported[3]. BDBA (0.25 g, 1.508 mmol) were added in a 1,4-dioxane / mesitylene mixture solution (1:1 v/v, 10 mL) with stirring for 30 min to form a homogeneous solution at room temperature, then the solution was transferred to a 25 ml Teflon-lined autoclave and maintained at 393 K for 72 h. After cooling to room temperature, the white solid was collected with centrifugation, and washed with 1,4-dioxane (20 mL) for three times. Then dried under vacuum conditions for 12 h at room temperature.

Synthesis of COF-5. COF-5 was synthesized using a slightly modified method with previously reported[4]. HHTP (112 mg, 0.345 mmol), BDBA (86 mg, 0.52 mmol) and methanol (0.21 mL, 5.2 mmol) were added in a dioxane / mesitylene mixture solution (4:1 v/v, 43 mL) at room temperature and sonicated for 30 minutes under N_2 atmosphere. The solution in a 100 mL round bottom flask was heated to 363 K for 20 hours at an oil-bath oven with stirring under atmospheric pressure (N_2). After cooling to room temperature, the solid was isolated by centrifugation and washed three times in acetone (30 mL). Subsequently, the solid was dried under vacuum at room temperature for 12 h.

Synthesis of Cu-BTC. Cu-BTC was synthesized using a slightly modified method with previously reported[5]. $Cu(NO_3)_2 \cdot 3H_2O$ (14 mmol, 3.38 g) were dissolved in 75 mL deionized water, and stirred vigorously until a clear solution was obtained. H_3BTC (14 mmol, 2.94 g) were also dissolved in 75 mL ethanol, and mixed with the prepared $Cu(NO_3)_2$ solution. The mixture was placed in a 500 mL capacity Teflon-lined stainless steel autoclave and heated at 383 K for 18 h. After completion of reaction, the autoclave was cooled down to room temperature and the blue powder formed was centrifuged and washed with deionized water (30 mL×3); the powder obtained was dried overnight at 353 K in air.

Synthesis of MIL-101(Cr). MIL-101(Cr) was synthesized using a slightly modified method with previously reported[6]. $Cr(NO_3)_3 \cdot 9H_2O$ (4.0 g, 10 mmol) and H_2BDC (1.66 g, 10 mmol) were added in 50 mL deionized water to get a mixture. 0.58 mL of glacial acetic acid was charged and added into the mixture. After that, the mixture sonicated for 30 minutes at room temperature. Then, the mixture transferred into a 100 mL capacity Teflon-lined stainless steel autoclave and heated at 473 K for 8 h. After cooling to room temperature, the green solids washed successively with deionized water, DMF and ethanol (30 mL×3). The obtained solids were dried overnight at 453 K under vacuum.

Characterization. Powder X-ray diffraction (PXRD) data were collected on a PANalytical X'Pert X-ray diffractometer in reflection mode using Cu Kα (λ= 1.540598 Å) radiation at 1600 W (40 kV, 40 mA). The 2θ rangs from 2° to 50° as a continuous scan with a step size of 0.01313° at room temperature. Samples

were mounted on zero background sample holders by dropping powders from a spatula and then leveling the sample surface with a glass microscope slide. No sample grinding or sieving was used prior to analysis.

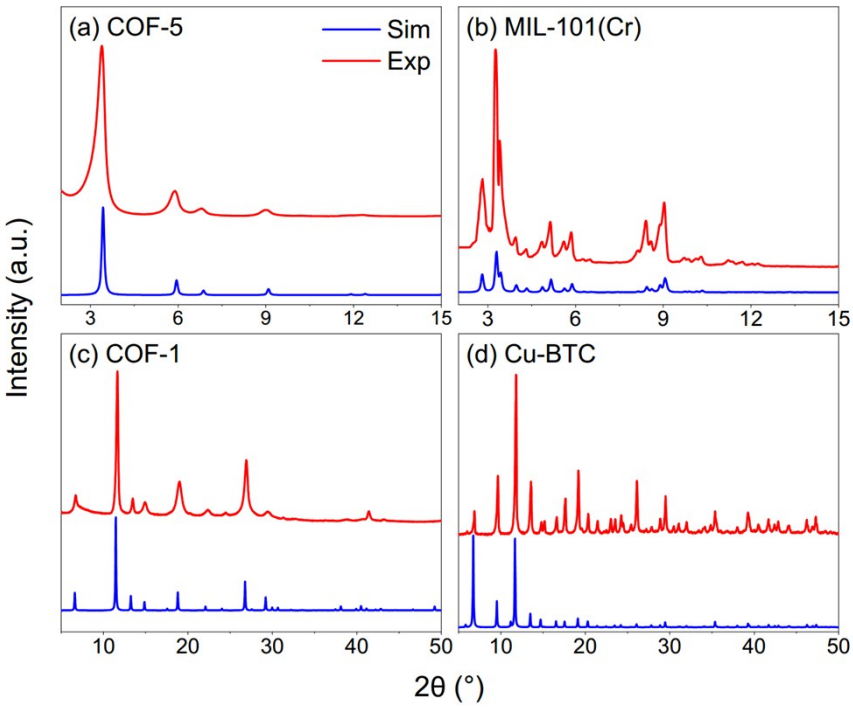

Fig. S14 Powder X-ray diffraction patterns of (a) COF-5, (b) MIL-101(Cr), (c) COF-1 and (d) Cu-BTC from experimental measurement and simulation.

Ethanol vapour adsorption. Ethanol vapor adsorption isotherms were measured at 288 and 298 K on an Autosorb-iQ2 from Quantachrome Instruments. In each measurement, absolute ethanol was added into vapor generator as the vapor source. Approximately 100 mg of samples were activated at 393 K for 24 h under vacuum. Adsorption isotherms were collected from P/P_0 = 0.01 to 0.9.

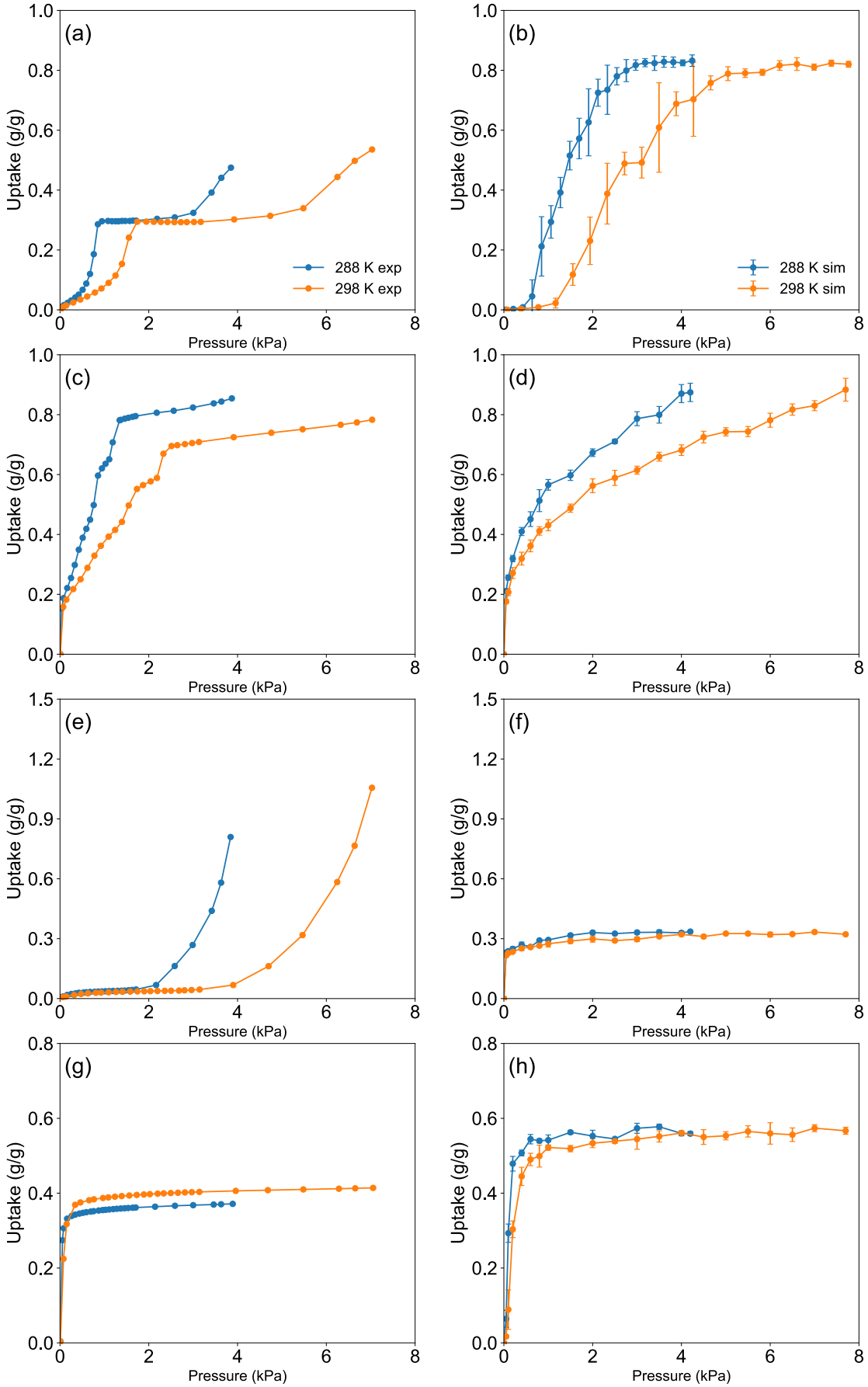

Fig. S15 Ethanol adsorption isotherms of (a) COF-5, (c) MIL-101(Cr), (e) COF-1 and (g) Cu-BTC in

experiment at 288 K and 298 K. The corresponding simulated ethanol adsorption isotherm of (b) COF-5, (d) MIL-101(Cr), (f) COF-1 and (h) Cu-BTC form GCMC simulation.

S6. Data mining and machine learning

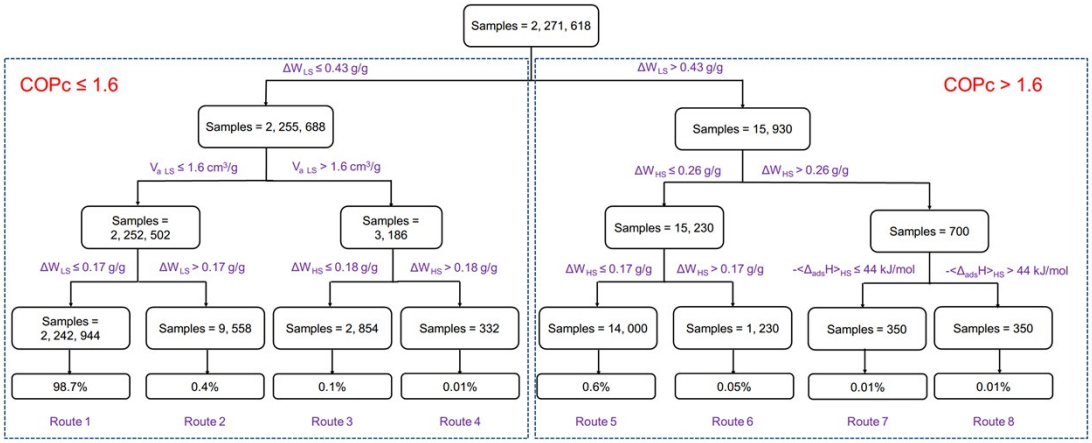

Fig. S16 The decision tree of type 1: MOF_{LS} + MOF_{HS}.

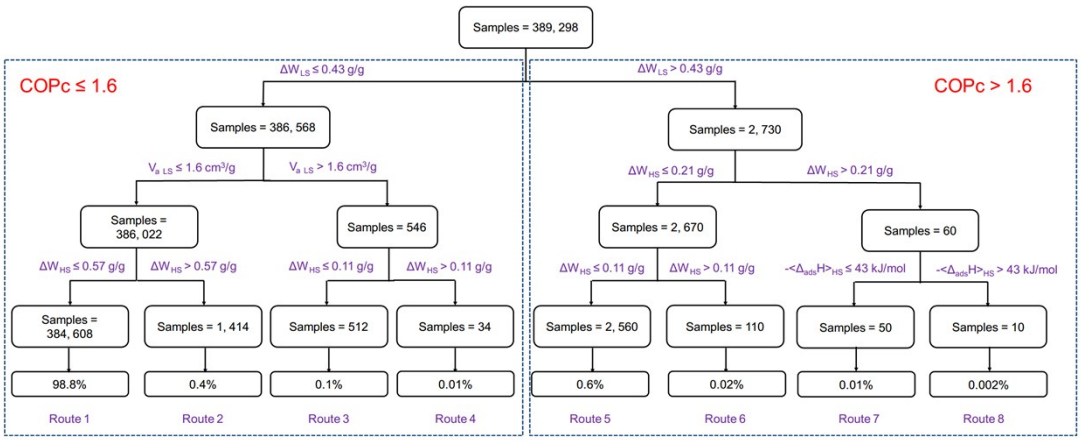

Fig. S17 The decision tree of type 2: MOF_{LS} + COF_{HS}.

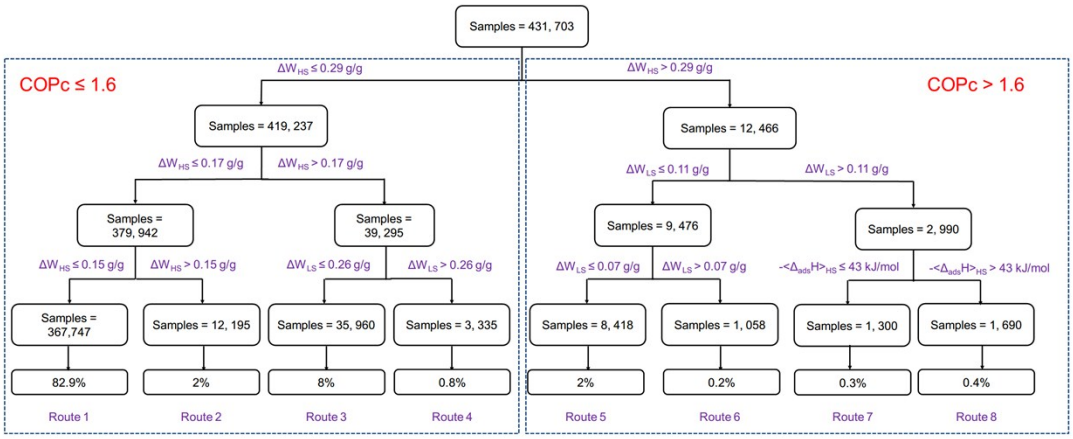

Fig. S18 The decision tree of type 3: COF_{LS} + MOF_{HS}.

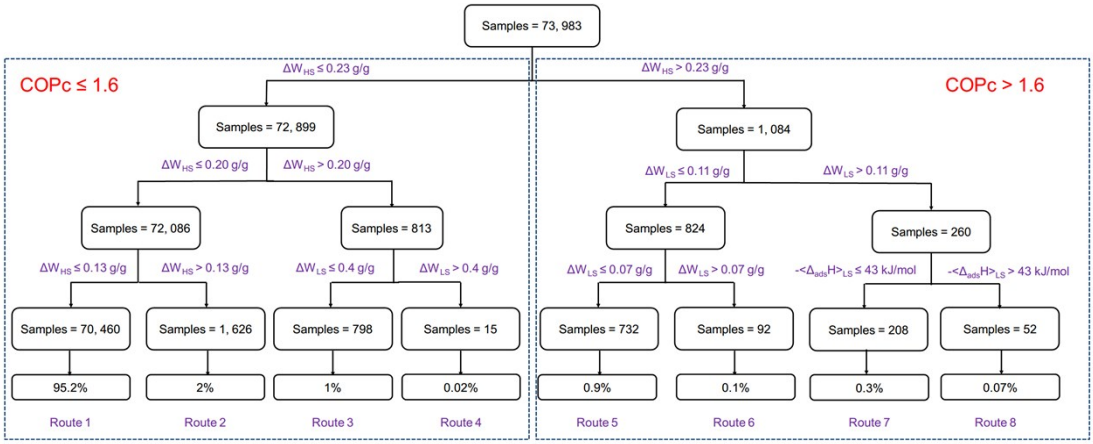

Fig. S19 The decision tree of type 4: COF_{LS} + COF_{HS}.

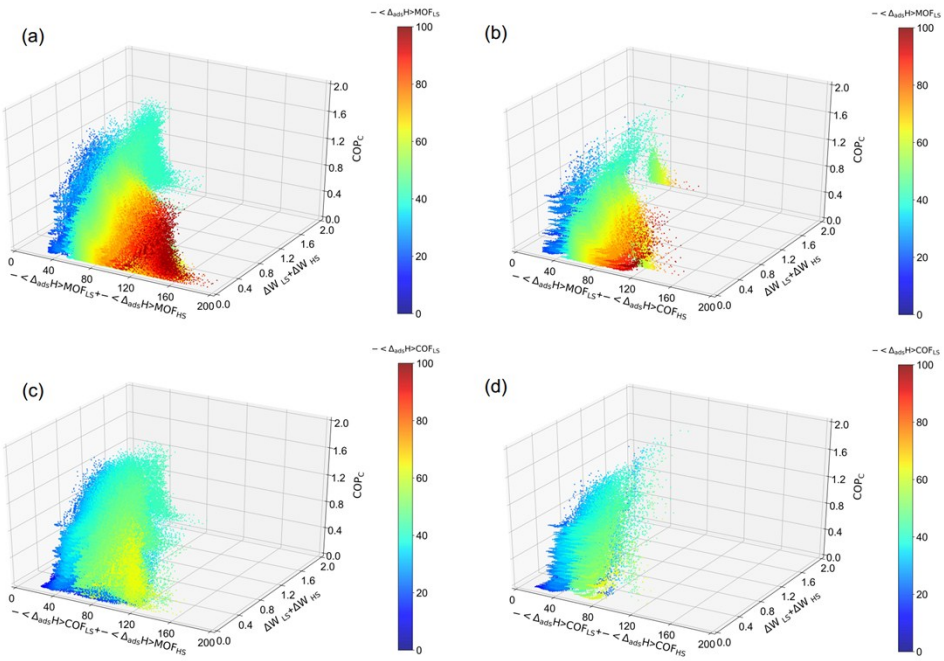

Fig. S20 The relationship between ΔW_{LS} + ΔW_{HS}, (-<Δ_{ads}H>$_{LS}$) + (-<Δ_{ads}H>$_{HS}$) and COP_C. (a) Type 1: MOFs for LS and HS (MOF_{LS} + MOF_{HS}). (b) Type 2: MOFs for LS and COFs for HS (MOF_{LS} + COF_{HS}). (c) Type 3: COFs for LS and MOFs for HS (COF_{LS} + MOF_{HS}). (d) Type 4: COFs for LS and HS (COF_{LS} + COF_{HS}).

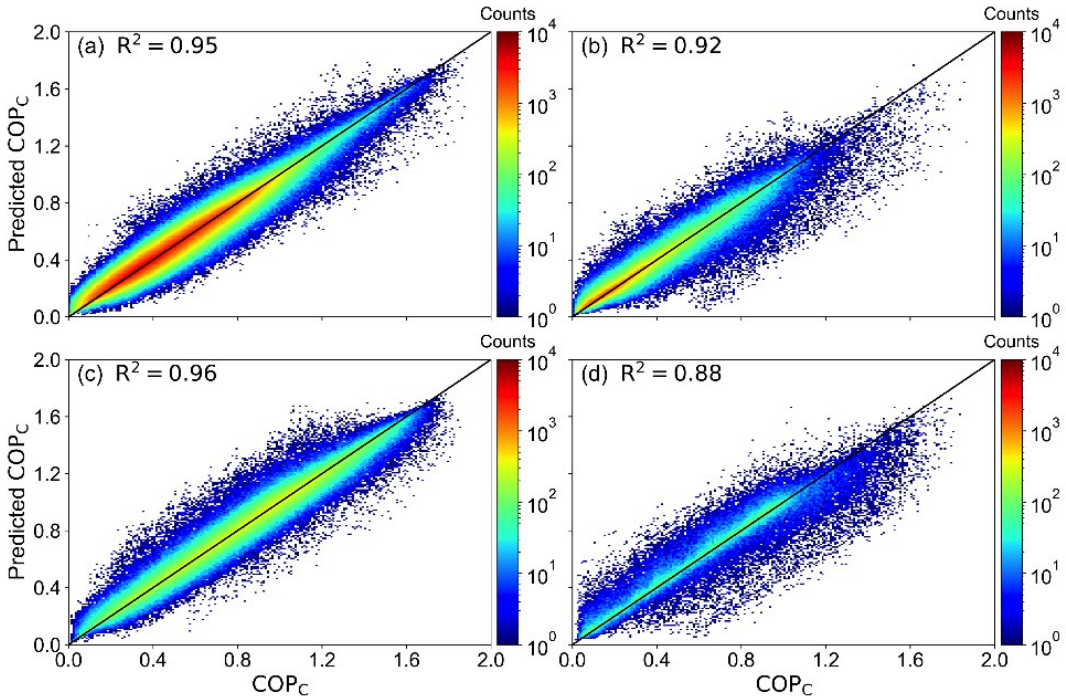

Fig. S21 The correlation between the COP_C and predicted COP_C in RF algorithms. (a) Type 1: MOFs for LS and HS (MOF_{LS} + MOF_{HS}). (b) Type 2: MOFs for LS and COFs for HS (MOF_{LS} + COF_{HS}). (c) Type 3: COFs for LS and MOFs for HS (COF_{LS} + MOF_{HS}). (d) Type 4: COFs for LS and HS (COF_{LS} + COF_{HS}).

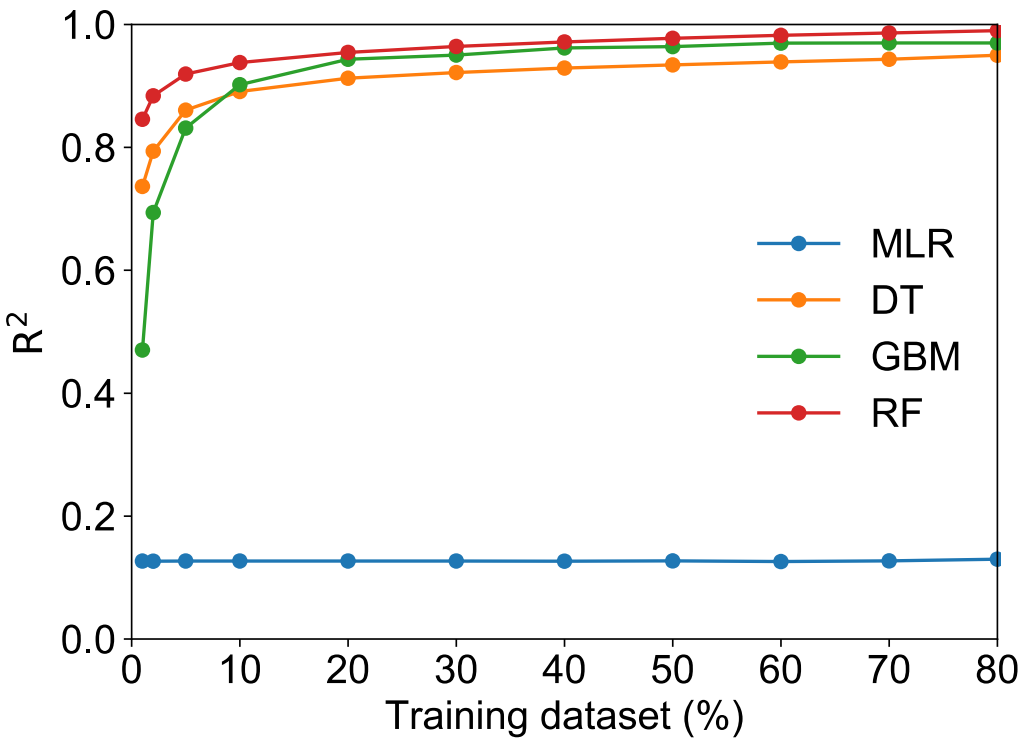

Fig. S22 The impacts of the percentage of training dataset on the prediction accuracy of machine learning algorithms of MLR, DT, GBM and RF.

References

1. R. Wang, L. Wang and J. Wu, *Adsorption refrigeration technology: theory and application*, John Wiley & Sons, Singapore, 2014.
2. Y. Liu and K. C. Leong, *International Journal of Refrigeration*, 2006, **29**, 250-259.
3. G. Li, K. Zhang and T. Tsuru, *ACS Applied Materials & Interfaces*, 2017, **9**, 8433-8436.
4. B. J. Smith and W. R. Dichtel, *Journal of the American Chemical Society*, 2014, **136**, 8783-8789.
5. Q. Min Wang, D. Shen, M. Bülow, M. Ling Lau, S. Deng, F. R. Fitch, N. O. Lemcoff and J. Semanscin, *Microporous and Mesoporous Materials*, 2002, **55**, 217-230.
6. P. B. S. Rallapalli, M. C. Raj, S. Senthilkumar, R. S. Somani and H. C. Bajaj, *Environmental Progress & Sustainable Energy*, 2016, **35**, 461-468.